


# Metabolite profiling in plasma and tissues of *ob/ob* and *db/db* mice identifies novel markers of obesity and type 2 diabetes

Pieter Giesbertz<sup>1,2</sup>  · Inken Padberg<sup>3</sup> · Dietrich Rein<sup>3</sup> · Josef Ecker<sup>1,2</sup> · Anja S. Höfle<sup>1,2</sup> · Britta Spanier<sup>1,2</sup> · Hannelore Daniel<sup>1,2</sup>

Received: 12 February 2015 / Accepted: 15 May 2015 / Published online: 10 June 2015  
© Springer-Verlag Berlin Heidelberg 2015

## Abstract

**Aims/hypothesis** Metabolomics approaches in humans have identified around 40 plasma metabolites associated with insulin resistance (IR) and type 2 diabetes, which often coincide with those for obesity. We aimed to separate diabetes-associated from obesity-associated metabolite alterations in plasma and study the impact of metabolically important tissues on plasma metabolite concentrations.

**Methods** Two obese mouse models were studied; one exclusively with obesity (*ob/ob*) and another with type 2 diabetes (*db/db*). Both models have impaired leptin signalling as a cause for obesity, but the different genetic backgrounds determine the susceptibility to diabetes. In these mice, we profiled plasma, liver, skeletal muscle and adipose tissue via semi-quantitative GC-MS and quantitative liquid chromatography (LC)-MS/MS for a wide range of metabolites.

**Results** Metabolite profiling identified 24 metabolites specifically associated with diabetes but not with obesity. Among these are known markers such as 1,5-anhydro-D-sorbitol, 3-hydroxybutyrate and the recently reported marker glyoxylate. New metabolites in the diabetic model were lysine, *O*-phosphotyrosine and branched-chain fatty acids. We also

identified 33 metabolites that were similarly altered in both models, represented by branched-chain amino acids (BCAA) as well as glycine, serine, *trans*-4-hydroxyproline, and various lipid species and derivatives. Correlation analyses showed stronger associations for plasma amino acids with adipose tissue metabolites in *db/db* mice compared with *ob/ob* mice, suggesting a prominent contribution of adipose tissue to changes in plasma in a diabetic state.

**Conclusions/interpretation** By studying mice with metabolite signatures that resemble obesity and diabetes in humans, we have found new metabolite entities for validation in appropriate human cohorts and revealed their possible tissue of origin.

**Keywords** Adipose tissue · Branched-chain amino acids · Insulin resistance · Liver · Metabolomics · Muscle

## Abbreviations

AAA	Aromatic amino acids
ADMA	<i>N,N</i> -dimethylarginine
BCAA	Branched-chain amino acids
BCKDH	Branched-chain keto acid dehydrogenase
FAS	Fatty acid synthase
IR	Insulin resistance
LC-MS	Liquid chromatography-MS
LPC	Lysophosphatidylcholine
PCA	Principal component analysis
SREBP	Sterol regulatory element-binding protein
TCA	Tricarboxylic acid

**Electronic supplementary material** The online version of this article (doi:10.1007/s00125-015-3656-y) contains peer-reviewed but unedited supplementary material, which is available to authorised users.

✉ Pieter Giesbertz  
pieter.giesbertz@tum.de

<sup>1</sup> Department of Nutritional Physiology, Technische Universität München, Gregor-Mendel-Str. 2, 85350 Freising, Germany

<sup>2</sup> ZIEL – Institute for Food & Health, 85350 Freising, Germany

<sup>3</sup> Metanomics Health GmbH and metanomics GmbH, Biomarker Program, Berlin, Germany

## Introduction

Metabolomics studies in humans have identified plasma metabolite signatures comprising around 40 entities that associate

with the development of insulin resistance (IR) and type 2 diabetes [1]. The most discriminating metabolites are the branched-chain (BCAA) and aromatic amino acids (AAA) as well as glycine and some other amino acid degradation products. Despite the fact that the changes in plasma BCAA and glycine have already been described by Felig et al as resulting from the ‘insulin ineffectiveness characteristic of obesity’ [2], the mechanisms leading to these changes are still not known. In addition to the amino acid markers, recent profiling studies have added numerous lipid species such as odd-chain fatty acids and various triacylglycerol species to the growing list of diabetes markers (for review see [3]).

A major confounder in studies on human IR and type 2 diabetes is obesity. Although most human studies in search of diabetes-derived metabolites are corrected for BMI, it is known that obesity and diabetes have multi-level associations. In this context, it is thus relevant to ask whether the identified plasma metabolites have just a reporter status or are also causative or at least contributing to IR or type 2 diabetes development and/or progression. This, for example, has been proposed for the BCAA, which increase in concentration in the obese state and appear to contribute to IR via a crosstalk of mechanistic target of rapamycin (mTOR) and insulin signalling pathways [4]. For a separation of obesity-related from diabetes-dependent changes we here describe findings employing mouse models for both conditions with assessment of metabolite changes in plasma and in insulin-sensitive tissues such as liver, muscle and adipose tissue, which may help to identify the origins of the plasma changes.

Both *ob/ob* and *db/db* mouse models have defective leptin signalling with a lack of leptin expression in *ob/ob* mice and a leptin-receptor deficiency in *db/db* mice. Most importantly, owing to their different genetic backgrounds, they possess different susceptibilities to develop diabetes. The *ob/ob* mice on the C57BL6/J background are able to compensate for IR and develop only a mild and transient hyperglycaemia associated with pancreatic hypertrophy and hyperplasia. In contrast, pancreatic tissue of *db/db* mice on the C57BLKS/J background undergoes atrophy resulting in a decline in insulin secretion and severe hyperglycaemia [5]. Coleman and Hummel showed that the difference in the mutation of the leptin-signalling components (either hormone or receptor) plays only a minor role in the susceptibility to develop diabetes [6]. Introduction of the *ob* mutation in mice with the C57BLKS/J background revealed the same strong diabetes phenotype as in C57BLKS/J mice with the *db* mutation. The *ob/ob* model thus develops obesity and milder IR but is rather resistant to diabetes, whereas the *db/db* model develops both obesity and diabetes with loss of beta cells. We used both models with animals matched by age and sex, and fed identical diets for 12 weeks for comparative metabolite profiling. We identified various previously described marker metabolites and also new compounds which we classified as ‘caused

by obesity with normoglycaemia’ or ‘caused by diabetes with severe hyperglycaemia’.

## Methods

**Animals** Male *db/db* mice and C57BLKS/J wild-type littermates ( $n=6-10$  per group) were purchased from Charles River Laboratories (Sulzfeld, Germany). Male *ob/ob* mice and C57BL6/J wild-type littermates ( $n=6-10$  per group), bred at the Research Center of Nutrition and Food Sciences (ZIEL), were obtained at the age of 5 weeks. Mice were kept on a standard-chow diet (ssniff V1534-0 R/M-H) for 3 weeks and were then placed on a chemically defined control diet (CCD; ssniff E15000-04 EF R/M Kontrolle) for 12 weeks. All mice had ad libitum access to food and water and were housed in the same open mouse facility. Body weight was determined weekly, and blood glucose was measured shortly before the end of the feeding trial. Animals were killed in a non-fasted state at an age of 20 weeks. Animal handling was conducted according with the Principles of Laboratory Care and was approved by the Veterinary Inspection Services.

**Plasma and tissue collection** Blood was collected into EDTA-coated tubes via cardiac puncture and centrifuged at 1,200 g and at 4°C to separate plasma. Plasma and tissues (liver, quadriceps muscle and epididymal adipose tissue) were collected, snap-frozen in liquid nitrogen, and stored at -80°C. Frozen tissues were ground prior to extraction of metabolites.

**Sample preparation and metabolite profiling of mouse samples** Broad metabolite profiling of plasma, liver, muscle and adipose tissue was performed using GC-MS (Agilent 6890 GC coupled to an Agilent 5973 MS System, Agilent, Waldbronn, Germany) and liquid chromatography-tandem MS (LC-MS/MS; Agilent 1100 HPLC, API 4000, Applied Biosystems, Darmstadt, Germany). In addition, for quantitative amino acid profiling of plasma, liver and muscle tissue, targeted LC-MS/MS (AB SCIEX QTrap 3200 LC-MS/MS System, AB SCIEX, Framingham, MA, USA) was applied using the aTRAQ Reagent Kit (Applied Biosystems, Darmstadt, Germany). Samples were analysed in a blinded and randomised analytical sequence design. See Electronic Supplementary Material (ESM) [Methods](#) for details on sample preparation and metabolite profiling.

**Data analysis and metabolite selection** Plasma metabolite concentrations in *ob/ob* and *db/db* mice were compared with their respective wild-type background and significantly changed metabolites were calculated by computing ANOVA models and using Student’s *t* statistics (unpaired and unequal variance). A significance threshold of  $\alpha < 0.05$  was applied. Adjustment of *p* values according to Benjamini and

Hochberg was applied to correct for multiple testing. Metabolites were categorised based on their significance level in both mouse models or their specific change in either of the models compared with respective wild-type mice.

We used principal component analysis (PCA) to identify the major metabolite groups in the plasma data. Subsequent *k*-means clustering on the five principal components identified 15 major metabolite groups in plasma. Refinement of the clustering results was done by bootstrapping the *k*-means clustering algorithm 20 times. The overall significance of each cluster between *ob/ob* and C57BL6/J mice, and between *db/db* and C57BLKS/J mice, was determined by combining the *p* values from each metabolite derived from the comparison of concentrations between knockout and wild-type groups using Fisher's combined probability test. Finally, correlation networks for every cluster were calculated using pairwise correlations based on the metabolite concentrations in plasma and corresponding metabolite concentrations in tissues. The statistical software environment *R* was used for calculations and network visualisations [7] applying the packages 'FactoMineR', 'fpc', 'MADAM' and 'qgraph'. No animals, samples or data were excluded from the reporting.

**Quantitative measurement of phospholipids in human plasma** Phospholipids and sphingomyelins were measured in samples from human prediabetics and healthy controls using flow injected MS (MS/MS, QTRAP5500, AB SCIEX, Framingham, MA, USA). All participants gave written informed consent and the investigations have been approved by the ethics committee of the Technische Universität München (protocol 2436/09). See Hoefle et al [8] and ESM Methods for further details.

**RNA isolation and quantitative real-time PCR analysis** RNA isolation and relative quantification of mRNA expression was performed as described previously with a few modifications [9]. See ESM Methods for further details and ESM Table 1 for applied primers.

## Results

**Phenotypic characterisation of *ob/ob* and *db/db* mice and PCA of metabolite profiles** Over 12 weeks of feeding, a dramatic weight gain was observed in both knockout mouse groups (Fig. 1a). Blood glucose concentrations were only increased in *db/db* mice (Fig. 1b) and plasma insulin levels were increased up to 35-fold in *ob/ob* mice and 2.5-fold in *db/db* mice compared with wild-type animals (Fig. 1c). Furthermore, increases in liver and adipose tissue mass and decreases in muscle mass were observed in both *ob/ob* and *db/db* mice (Fig. 1d–f).

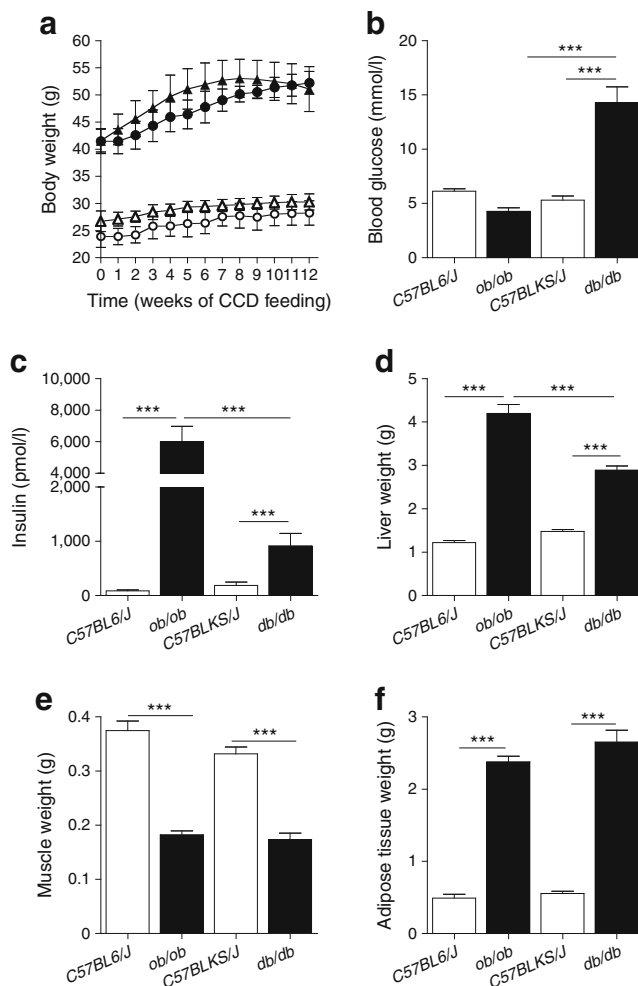


**Fig. 1** Phenotypic characteristics of *ob/ob*, *db/db* and wild-type control mice. (a) Body weight development over the feeding period. White and black symbols represent wild-type and knockout mice, respectively. Circles and triangles represent C57BL6/J and C57BLKS/J mice, respectively. (b) Blood glucose concentrations of the 20-week-old animals and (c) plasma insulin concentrations at week 20. (d) Total weight of all liver lobes. (e) Total weight of left and right quadriceps muscles. (f) Total weight of left and right epididymal adipose tissue depots. Data are presented as means±SEM. \*\*\**p*<0.001

PCA of plasma and tissue metabolite profiles showed a close relationship between wild-type mice from both groups (Fig. 2), while both knockout groups separated from wild-type groups and from each other (for plasma and adipose tissue, in the first and second dimensions; and for liver, in the second dimension). Muscle tissue of wild-type strains separated in the second dimension (not shown), while knockout animals differentiated in the third dimension.

**Plasma metabolite changes** From the 170 metabolites quantified in plasma, 33 metabolites changed significantly in both *ob/ob* and *db/db* mice compared with respective wild-type animals (Table 1). Except for serine, changes in plasma concentrations remained significant after adjustment for multiple

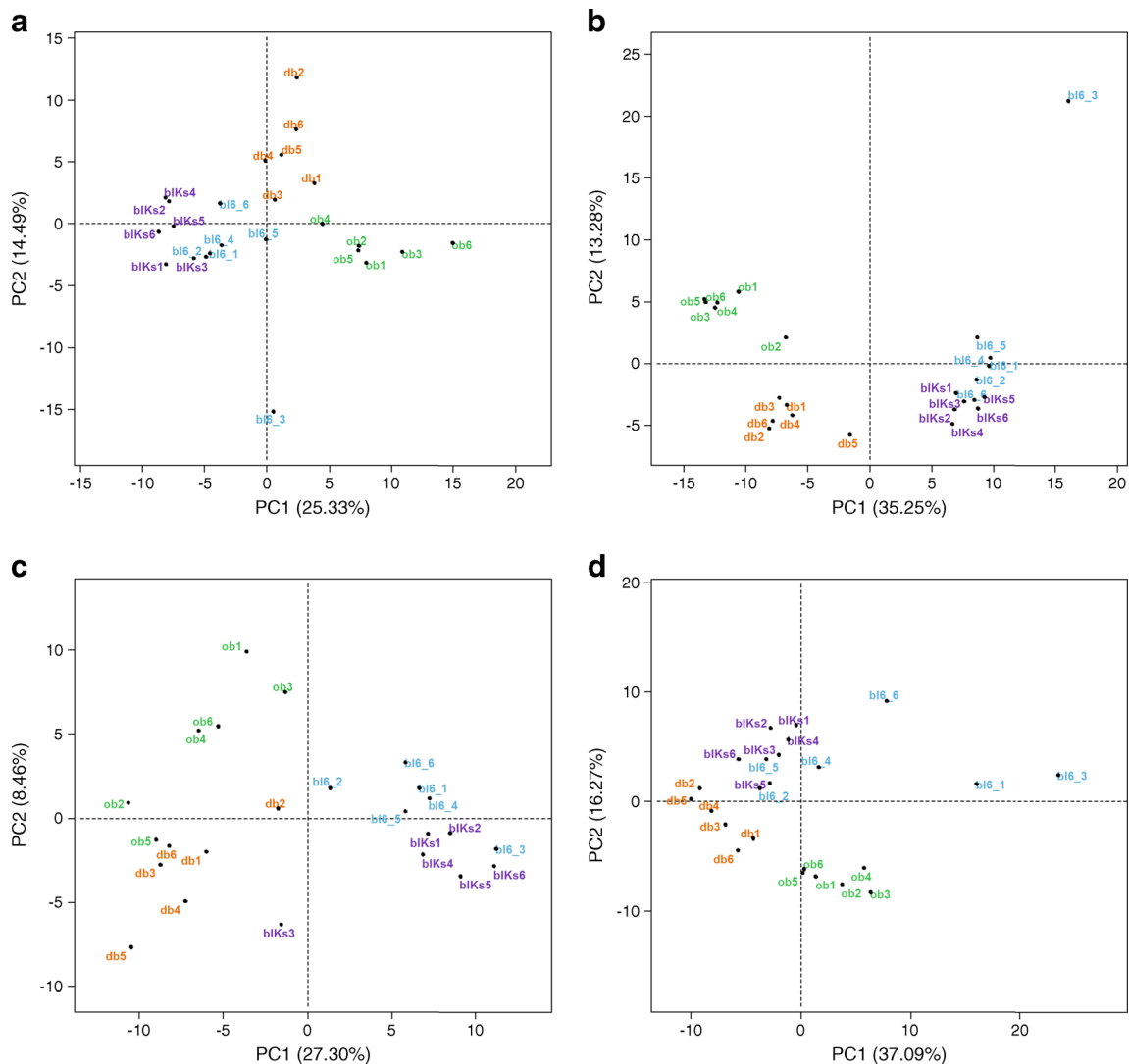


**Fig. 2** PCA of metabolite profiles from plasma and tissues. **(a)** Plasma; **(b)** liver; **(c)** muscle; **(d)** adipose tissue. bl6, wild-type mice with C57BL/6J background; bIKs, wild-type mice with C57BLKS/J background; PC, principal component

testing. Prominent increases were observed for metabolites from diverse lipid classes, such as polyunsaturated fatty acids, (lyso)phosphatidylcholines, sphingomyelins and fatty alcohols as well as cholesterol and some cholesteryl ester species, while behenic acid (C22:0) was decreased. Common increases were also observed for BCAA and leucine-derived  $\alpha$ -ketoisocaproic acid, while glycine, serine and *trans*-4-hydroxyproline levels were decreased. These metabolites thus seem to change in the early phases of IR and type 2 diabetes but mostly as a consequence of obesity.

Twenty-four metabolites changed specifically in the plasma of *db/db* mice (Table 2), of which 12 remained significant after *p* value adjustment. Besides increases in glucose, elevated levels of glyoxylate were found, which we recently described as a diabetes marker [10]. In addition, corticosterone and 18-hydroxy-11-deoxycorticosterone concentrations were markedly elevated. Specific increases were also found for the

branched-chain fatty acids 16-methylheptadecanoic acid and 3-hydroxyisobutyrate, as well as for *O*-phosphotyrosine, while lysine, arginine and lignoceric acid (C24:0) were decreased. Specific increases in *db/db* mice were also found for phospholipids containing linoleic acid. Strong trends for changes in plasma concentrations of *N,N*-dimethylarginine (ADMA) and 3-hydroxybutyrate were found, suggesting a mild ketogenic condition.

In plasma of *ob/ob* mice, 35 metabolites changed significantly (ESM Table 2). Of those, 24 remained significant after *p* value adjustment, comprising even-numbered fatty acids in unesterified forms and in ceramides, phospholipids, sphingolipids and cholesteryl esters with major increases, while triacylglycerols were reduced. Interestingly, whereas various branched-chain fatty acids were elevated in *db/db* mice, decreases of branched-chain isopalmitic acid and odd-chain C17:0 lysophosphatidylcholine were found in *ob/ob*

**Table 1** Plasma metabolites significantly changed in both *ob/ob* and *db/db* mice

Metabolite	<i>ob/ob</i> vs C57BL6/J			<i>db/db</i> vs C57BLKS/J		
	Ratio <i>ob</i> :WT <sup>a</sup>	<i>p</i> value	Adjusted <i>p</i>	Ratio <i>db</i> :WT	<i>p</i> value	Adjusted <i>p</i>
Acyl-carriers and related						
Pantothenic acid	1.82	0.008	0.029	1.67	0.016	0.061
Amino acids, neutral						
Glycine	0.56	0.001	0.005	0.60	1.96×10 <sup>-4</sup>	0.002
Serine	0.83	0.019	0.053	0.77	0.016	0.060
BCAA-related						
α-ketoisocaproic acid	1.44	0.029	0.077	1.97	2.08×10 <sup>-4</sup>	0.002
Valine	1.44	9.81×10 <sup>-5</sup>	0.001	1.58	6.16×10 <sup>-5</sup>	0.001
Leucine	1.48	5.73×10 <sup>-5</sup>	0.001	1.59	4.96×10 <sup>-4</sup>	0.004
Isoleucine	1.51	1.34×10 <sup>-5</sup>	2.47×10 <sup>-4</sup>	1.62	0.002	0.013
Cholesterol and related						
Cholesterol, total	2.00	5.63×10 <sup>-6</sup>	1.37×10 <sup>-4</sup>	1.90	1.01×10 <sup>-6</sup>	3.42×10 <sup>-5</sup>
Cholesterol, free	1.64	3.00×10 <sup>-4</sup>	0.003	1.51	0.002	0.012
Cholesteryl ester C20:4	1.87	0.003	0.015	1.87	0.003	0.020
Collagen metabolism						
Hydroxyproline	0.42	4.61×10 <sup>-4</sup>	0.004	0.32	3.79×10 <sup>-4</sup>	0.003
Dipeptides						
Anserine	0.34	0.014	0.046	0.39	0.008	0.038
Fatty acids, polyunsaturated						
Eicosapentaenoic acid (C20: <i>cis</i> [5,8,11,14,17]5)	2.81	1.49×10 <sup>-6</sup>	8.21×10 <sup>-5</sup>	3.24	2.67×10 <sup>-8</sup>	4.40×10 <sup>-6</sup>
Arachidonic acid (C20: <i>cis</i> [5,8,11,14]4)	2.87	3.83×10 <sup>-7</sup>	3.56×10 <sup>-5</sup>	2.34	5.47×10 <sup>-7</sup>	3.42×10 <sup>-5</sup>
Dihomo-γ-linolenic acid (C20: <i>cis</i> [8,11,14]3)	3.09	4.31×10 <sup>-7</sup>	3.56×10 <sup>-5</sup>	2.36	1.24×10 <sup>-6</sup>	3.42×10 <sup>-5</sup>
Fatty acids, saturated						
Stearic acid (C18:0)	2.20	3.54×10 <sup>-6</sup>	1.21×10 <sup>-4</sup>	2.04	1.24×10 <sup>-6</sup>	3.42×10 <sup>-5</sup>
Behenic acid (C22:0)	0.50	0.002	0.008	0.66	0.012	0.053
Phospholipids						
LPC (C20:4)	1.27	0.001	0.005	1.30	3.60×10 <sup>-4</sup>	0.003
LPC (C18:1)	1.20	0.001	0.005	1.18	0.002	0.013
LPC (C18:0)	1.14	0.046	0.114	1.19	0.011	0.048
PC (C18:1,C18:2) or PC (C16:0,C20:3)	1.08	0.005	0.019	1.15	8.92×10 <sup>-6</sup>	1.84×10 <sup>-4</sup>
PC (C18:0,C20:4)	1.21	3.30×10 <sup>-4</sup>	0.003	1.27	3.83×10 <sup>-5</sup>	0.001
PC (C16:0,C16:0)	0.71	0.002	0.010	0.62	7.92×10 <sup>-5</sup>	0.001
PC (C18:0,C20:3) or PC (C20:1,C18:2) or PC (C20:2,C18:1)	1.66	6.47×10 <sup>-6</sup>	1.37×10 <sup>-4</sup>	1.49	1.07×10 <sup>-4</sup>	0.001
PC (C16:0,C20:5)	1.46	0.007	0.028	1.39	0.018	0.064
PC (C18:0,C18:1)	1.24	0.001	0.005	1.12	0.045	0.131
Glycerol phosphate, lipid fraction	2.43	2.67×10 <sup>-5</sup>	4.41×10 <sup>-4</sup>	1.82	2.11×10 <sup>-4</sup>	0.002
Polyols						
1,5-Anhydrosorbitol	0.18	0.001	0.006	0.03	8.15×10 <sup>-7</sup>	3.42×10 <sup>-5</sup>
Redox-carrier and related						
Coenzyme Q9	7.78	6.66×10 <sup>-6</sup>	1.37×10 <sup>-4</sup>	3.26	0.002	0.013
Sphingomyelins						
Sphingomyelin (d18:2,C18:0)	1.53	0.001	0.005	1.46	0.002	0.013
Sphingomyelin (d18:1,C16:0)	1.21	2.09×10 <sup>-4</sup>	0.002	1.11	0.023	0.077
Tocopherols and related						
α-Tocopherol	1.70	0.006	0.023	1.57	0.015	0.060
Triacylglycerols						
TAG (C18:2,C18:3)	0.31	0.015	0.046	0.39	0.042	0.125

<sup>a</sup> Metabolite changes are expressed as ratios of metabolite concentrations in knockout mice compared with the respective control mice

PC, phosphatidylcholine; TAG, triacylglycerol; WT, wild-type

**Table 2** Plasma metabolites significantly changed solely in *db/db* mice

Metabolite	<i>ob/ob</i> vs C57BL6/J		<i>db/db</i> vs C57BLKS/J		
	Ratio <i>ob</i> :WT <sup>a</sup>	<i>p</i> value	Ratio <i>db</i> :WT	<i>p</i> value	Adjusted <i>p</i>
Amino acids, neutral					
Asparagine	1.01	n.s.	0.76	0.041	0.124
Ascorbic acid and related					
Threonic acid	1.25	n.s.	1.61	0.017	0.064
BCAA metabolism					
3-Hydroxyisobutyrate	0.92	n.s.	1.64	0.020	0.067
Citrate cycle					
Succinate	0.94	n.s.	0.89	0.039	0.120
Creatine metabolism					
Creatinine	0.72	n.s.	0.64	0.037	0.117
Fatty acids, branched					
16-Methylheptadecanoic acid	0.84	n.s.	1.47	0.004	0.021
Fatty acids, polyunsaturated					
Linoleic acid (C18: <i>cis</i> [9,12]2)	0.97	n.s.	1.39	0.014	0.059
Fatty acids, saturated					
Lignoceric acid (C24:0)	0.74	n.s.	0.59	0.005	0.022
Glycolipids					
Glucose, lipid fraction	1.52	n.s.	1.69	0.045	0.131
Glycolysis/gluconeogenesis					
Glucose-6-P or fructose-6-P or myo-inositol-P	1.20	n.s.	2.15	0.004	0.021
Lactaldehyde	1.01	n.s.	0.66	0.031	0.101
Ketone bodies					
3-Hydroxybutyrate	1.19	n.s.	1.84	0.014	0.059
Lipid precursors					
Glycerol, polar fraction	1.04	n.s.	1.37	0.015	0.060
Lysine metabolism					
$\alpha$ -Aminoadipic acid	0.83	n.s.	0.69	0.021	0.072
Lysine	1.14	n.s.	0.66	0.002	0.013
Miscellaneous					
Glyoxylate	1.47	n.s.	6.06	$6.18 \times 10^{-5}$	0.001
Monosaccharides					
Glucose or galactose or gluconic acid or mannitol	1.72	n.s.	4.81	$8.06 \times 10^{-6}$	$1.84 \times 10^{-4}$
Other hormones					
ADMA	1.00	n.s.	0.71	0.019	0.066
Phospholipids					
Lysophosphatidylcholine (C18:2)	0.95	n.s.	1.41	$1.60 \times 10^{-4}$	0.002
PC (C16:0,C20:4) or PC (C18:2,C18:2)	1.01	n.s.	1.03	0.006	0.029
Steroids and related					
18-Hydroxy-11-deoxycorticosterone or 11-deoxycortisol	1.50	n.s.	7.18	0.002	0.013
Corticosterone	1.48	n.s.	4.93	0.004	0.022
Tyrosine metabolism					
<i>O</i> -phosphotyrosine	0.92	n.s.	1.96	0.004	0.021
Urea cycle					
Arginine	0.74	n.s.	0.59	$2.49 \times 10^{-5}$	$4.57 \times 10^{-4}$

<sup>a</sup> Metabolite changes are expressed as ratios of metabolite concentrations in knockout mice compared with the respective control mice  
n.s., not significant; PC, Phosphatidylcholine

mice. Specific increases of phenylalanine and tryptophan levels were also observed in *ob/ob* animals, while tryptophan

breakdown-products kynurenic acid and xanthurenic acid were reduced. In contrast, indole-3-propionic acid and

3-indoxylsulfate, arising from bacterial tryptophan breakdown [11], increased in plasma. Moreover, *ob/ob* mice displayed strong increases in ornithine and decreases in  $\alpha$ -aminobutyrate concentrations in plasma.

**Metabolite changes in liver, quadriceps muscle and epididymal adipose tissue** Metabolite profiles were obtained from liver, quadriceps muscle and epididymal adipose tissue as metabolically important and insulin-dependent organs. An overview of hepatic metabolite concentration changes in *ob/ob* and *db/db* animals compared with respective wild-type animals is shown in ESM Fig. 1a,b. Metabolites from different lipid classes were dramatically increased in both models with stronger increases in *ob/ob* mice, while very-long-chain fatty acid levels were decreased (ESM Fig. 1a). Furthermore, both models displayed increased BCAA and reduced glycine and *trans*-4-hydroxyproline concentrations. Most pronounced differences in liver between *ob/ob* and *db/db* mice were found for pentoses and intermediates of the pentose phosphate pathway with increases in *db/db* mice and decreases in *ob/ob* mice (ESM Fig. 1b).

ESM Fig. 1c,d show metabolite concentration changes in muscle tissue in the two knockout mouse groups compared with the respective control mice. Both models displayed strongest elevations in free long-chain fatty acids, represented by straight-, branched- and odd-chain forms, with a more pronounced increase in the *ob/ob* group (ESM Fig. 1c). In contrast to liver tissue, no changes were observed for phospholipids. Marked differences between *ob/ob* and *db/db* groups were found for intermediates of the glycolytic chain comprising fructose-6-phosphate, fructose-1,6-diphosphate, glucose-6-phosphate and 3-phosphoglycerate, which all increased dramatically in *ob/ob* but only modestly in *db/db* mice (ESM Fig. 1d).

Adipose tissue displayed a strong decrease in levels of saturated very-long-chain fatty acids in both models (ESM Fig. 1e). Other fatty acids—in particular monounsaturated and polyunsaturated species—had increased concentrations. Furthermore, the tricarboxylic acid (TCA) cycle intermediates malate and fumarate were increased. Cholesterol showed increased concentrations in *ob/ob* mice and decreased concentrations in *db/db* mice (ESM Fig. 1f).

**Identification of principal metabolite groups in plasma** PCA, with subsequent clustering on principal components, identified 15 metabolite clusters in plasma. Metabolites clustered into groups with biochemical similarity or with common metabolic pathways. ESM Table 3 displays the overall significance of the clusters reached for the two knockout models as compared with wild-type mice. Five metabolite clusters displayed high significance for both knockout models (clusters 4, 8, 10, 13, 15), consisting of phospholipids, triacylglycerols, AAA and BCAA, as well as glycine,

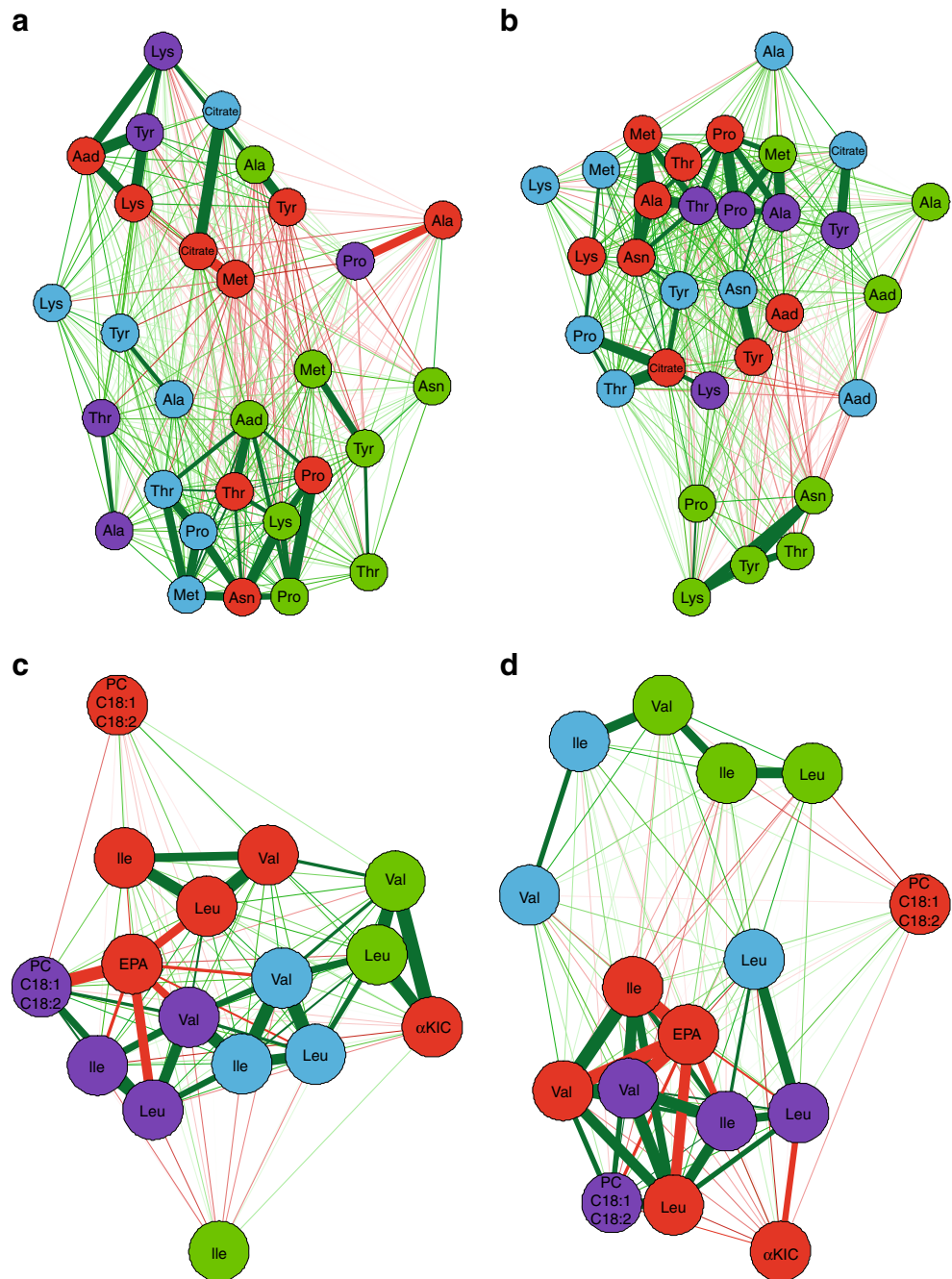
histidine and *trans*-4-hydroxyproline. Interestingly, four clusters (clusters 1, 5, 9, 11)—mainly consisting of amino acids, hexoses and catabolites—showed overall significant changes only between *db/db* and C57BLKS/J wild-type mice. Similarly, two clusters (clusters 3 and 6) showed an overall significant change only between *ob/ob* and corresponding control mice. These clusters consisted of fatty acids, TCA cycle intermediates and cholesteryl esters.

**Correlation networks of plasma and tissue metabolites** To explore which tissue contributes most to the changes in blood metabolites, correlation networks for every metabolite cluster between plasma and the different organs were calculated. Selected networks are displayed in Fig. 3. Clearest differences between the correlation networks of *ob/ob* and *db/db* mice were obtained for clusters 11 and 13 containing amino acids. For cluster 11, especially adipose tissue correlated strongly with plasma in the *db/db* model, while correlations with liver metabolites remained weak. In the *ob/ob* model, in contrast, liver revealed much stronger correlations. The same interdependence was observed for cluster 13, containing the BCAA. Most distinct was the network for the *db/db* model revealing strong positive correlations for BCAA between plasma and adipose tissues while correlations with liver were weak. The product of leucine transamination,  $\alpha$ -ketoisocaproic acid, correlated negatively with adipose tissue leucine content. In contrast, in *ob/ob* mice,  $\alpha$ -ketoisocaproic acid correlated strongest in a positive manner with liver. The observed clustering suggests an important contribution of adipose tissue to plasma amino acid concentrations in the *db/db* and far less so in the *ob/ob* model, whereas the liver appears to exert more influence in the *ob/ob* model.

## Discussion

Obesity, IR and type 2 diabetes in humans cause significant changes in an array of plasma metabolites of which some have the quality to predict diabetes development in early phases [1]. In mouse models mimicking the human conditions of type 2 diabetes development, we assessed which metabolite changes associate mainly with obesity and which are specific for the diabetic state. Despite a common obesity phenotype, the mice display different impairments in glucose homeostasis and beta cell function resembling an obese phenotype with a mild IR (*ob/ob*) or a fully developed type 2 diabetes (*db/db*). By using appropriate wild-type mice as controls, we eliminated putative effects of the different genetic backgrounds. In addition to plasma, we generated metabolite profiles of liver, muscle and adipose tissue as an explorative approach which could provide indications on the origins of plasma metabolite changes. With this strategy, metabolites were identified that changed in concentrations in both the *ob/ob* and the *db/db* mice when

**Fig. 3** Correlation networks of selected metabolite clusters. (**a,b**) Correlation networks for metabolite cluster 11 (see ESM Table 3) for *ob/ob* (**a**) and *db/db* (**b**) mice. (**c,d**) Correlation networks for metabolite cluster 13 for *ob/ob* (**c**) and *db/db* (**d**) mice. Node colours indicate tissue type (red, plasma; green, liver; blue, muscle; purple, adipose tissue). Green and red line colours indicate positive and negative correlations, respectively. Line thickness represents the strength of the correlation, with thicker lines indicating stronger correlations. Aad,  $\alpha$ -amino adipic acid; EPA, eicosapentaenoic acid; KIC,  $\alpha$ -ketoisocaproic acid; PC, principal component



compared with their respective wild-type background, and we also found metabolites that specifically mark the obese state without diabetes or the diabetic state on a background of obesity.

In addition, we compared metabolite changes in mice with alterations observed in two independent human studies comprising either prediabetic or diabetic individuals (ESM Tables 4 and 5). Prediabetic participants were defined by the WHO's criteria and diabetic patients were defined according to self-reporting, and/or type-2 diabetes medication, and/or  $HbA_{1c} > 6.5\%$  (47.5 mmol/mol) and fasting plasma glucose

levels  $> 5.55$  mmol/l. While parts of both studies were recently published [8, 12], we focused on novel metabolite measurements from these studies and could identify similar changes in human plasma for various known but also several yet undescribed metabolites. Interestingly, while most changes in phospholipid concentrations of prediabetic individuals were concordant with the alterations in both *ob/ob* and *db/db* mice, metabolite profiles of diabetic individuals showed strongest similarities to *db/db* mice, substantiating the discriminant power of the specific alterations observed in plasma from mice in this study.



**Common alterations in lipid profiles reflect changes in de novo lipogenesis as a consequence of impaired leptin and insulin signalling** Most pronounced in both models were increases in long-chain fatty acids and corresponding phospholipids, in plasma and predominantly in liver. It is well established that hepatic de novo lipogenesis is increased in obese and IR states leading to non-alcoholic fatty liver disease (NAFLD) [13]. Leptin is known to suppress stearoyl-CoA desaturase (SCD-1) which catalyses the synthesis of monounsaturated fatty acids [14]. The primary lack of leptin signalling in both mouse models may thus explain the observed increases in hepatic palmitoleic and oleic acid levels. Insulin controls de novo lipogenesis and both models are hyperinsulinaemic, which in turn affects liver as an insulin-dependent organ. Despite a developing IR, the hepatic sterol regulatory element-binding protein (SREBP)-1c signalling pathway remains insulin sensitive [15]. Increases in hepatic levels of long-chain fatty acids, polyunsaturated fatty acids and related phospholipids may well reflect changes of enzymes encoded by SREBP-1-dependent genes [16]. Remarkably, most saturated and monounsaturated fatty acids of 20–24 carbon units decreased in plasma, liver and adipose tissue, which could be a consequence of altered elongase-1 levels, the prime enzyme in the production of very-long-chain fatty acids [17]. Increased levels of isopentenyl pyrophosphate suggest enhanced hepatic cholesterol synthesis, regulated by SREBP-1a [18] and SREBP-2 [19].

Skeletal muscle also showed strong increases in concentrations of long-chain fatty acids in *ob/ob* and *db/db* mice. Although muscle tissue is not thought to significantly contribute to overall lipid production, ectopic lipid accumulation is associated with IR and NEFA in tissues, including muscle, and is thought to cause lipotoxicity and promote IR. Although increased fatty acid levels may indicate a larger supply from plasma by enhanced adipose tissue lipolysis or decreased fatty acid clearance [20, 21], increased activity of muscle-specific fatty acid synthase (FAS) might also contribute to increased levels of fatty acids [22].

**Specific metabolite changes in *db/db* mice relate to hyperglycaemia and comorbidities** In contrast to *ob/ob* mice, *db/db* animals are highly hyperglycaemic with only modestly elevated insulin levels, reflecting the increased susceptibility of *db/db* mice to beta cell exhaustion [5]. The *db/db* mice displayed specific changes in plasma metabolites, which were previously reported as associated with hyperglycaemia and its comorbidities. Decreased ADMA levels, related to altered endothelial functions, were reported for type 2 diabetes [23]; and low plasma levels of 1,5-anhydrosorbitol that result from competitive inhibition of reabsorption via glucose transporters in kidney by the high load of filtered glucose are also known in type 2 diabetes [24]. Furthermore, glyoxylate, recently described as a new marker for diabetes [12], was

strongly increased in plasma of *db/db* mice. Decreased creatinine concentrations reflect a reduced muscle mass [25] here showing a stronger decrease in the *db/db* model. This is associated with increased muscle catabolism causing the observed rise in plasma amino acids and elevated glucocorticoid levels. Last, the increase in plasma *O*-phosphotyrosine might relate to elevated platelet activation as a result of the hyperglycaemic state [26, 27]. Most interestingly, phosphotyrosine appeared in the same cluster with glucose and glyoxylate (see ESM Table 3).

#### **Correlation networks and gene expression analysis suggest an increased role for adipose tissue in the *db/db* mice and for liver in *ob/ob* mice**

Both knockout models showed increased levels of BCAA and  $\alpha$ -ketoisocaproic acid, the transamination product of leucine, in plasma and tissues. Leptin and insulin both contribute to the maintenance of muscle protein [16, 28]. Disturbances in leptin signalling and IR in turn increase protein degradation in muscle releasing amino acids into circulation. While most amino acids are used for hepatic gluconeogenesis, BCAA show a different fate. A significant contribution of adipose tissue to the metabolism of BCAA has become obvious in recent years. In 2007, She et al showed a decreased protein level and activity of the mitochondrial branched-chain amino acid transferase (BCAT2) and the rate-limiting branched-chain keto acid dehydrogenase (BCKDH) complex in obese rodents [29]. The networks for the BCAA cluster (cluster 13, see Fig. 3c,d) showed strong correlations between plasma and adipose tissue in the *db/db* but not in *ob/ob* mice. However, analysis of mRNA levels in adipose tissue showed similar decreases in both knockout models for *Bckdha*, the gene encoding the E1 $\alpha$  component of the BCKDH complex, as well as for the kinase (*Bckdk*) and for the phosphatase (*Ppm1k*) regulating BCKDH activity, while *Bcat2* remained unchanged (see ESM Fig. 2). This finding suggests that, in mice, other tissues likely contribute to the changes in BCAA levels. A recent study describes the effects of insulin on hepatic protein levels and activity of BCKDH in controlling BCAA catabolism [30]. Since *ob/ob* mice are hyperinsulinaemic, the plasma BCAA concentrations may be influenced more strongly by hepatic BCKDH in *ob/ob* mice, which is also supported by the strong correlations of plasma  $\alpha$ -ketoisocaproic acid and hepatic BCAA in the correlation network of the *ob/ob* mice.

**Changes in branched-chain fatty acids may link to BCAA-derived precursors** Interestingly, plasma concentrations of odd-numbered and branched-chain fatty acids changed in different directions in the two mouse models. Whereas 16-methylheptadecanoic acid was specifically increased in *db/db* mice, *ob/ob* mice showed a decrease in C17

lysophosphatidylcholine (LPC C17:0) levels and a strong trend for a decrease for isopalmitic acid. In cohort studies, plasma levels of LPC C17:0 were recently reported to be reduced in type 2 diabetes patients [1, 31]. How odd-chain and branched-chain fatty acids link to IR and type 2 diabetes is currently not known. However, 3-hydroxyisobutyric acid, a branched short-chain fatty acid derived from valine breakdown, was specifically increased in *db/db* mice. As shown in rat epididymal adipose tissue, FAS can generate odd/branched long-chain fatty acids from propionyl-CoA and branched-chain C4- and C5-iso-acyl-CoAs as primers which are all intermediates of BCAA breakdown [32]. An aberrant availability of short-chain acyl-CoA primers for use in fatty acid synthesis could explain the changes in odd- and branched-chain fatty acid concentrations found in plasma in an insulin-resistant or diabetic state.

**Conclusion** We compared metabolite profiles in plasma and selected tissues of two mouse models with obesity but different stages of diabetes development. With this approach, we could define metabolites that change in the obese states and those that depend on insulin action and are associated with severe hyperglycaemia. Analysis of liver, muscle and adipose tissue revealed dominant changes in fatty acid and amino acid metabolism, with a more dominant role for adipose tissue in the diabetes model. We also identified new marker metabolites with significant changes in tissues and plasma and found similar changes for various metabolites in plasma from human prediabetic and diabetic volunteers.

**Acknowledgements** We thank M. Klingenspor and F. Bolze (Molecular Nutritional Medicine Unit, Technische Universität München, Freising, Germany) for *ob/ob* mice, and R. Scheundel (Nutritional Physiology Unit, Technische Universität München, Freising, Germany) for animal handling and sample collection. For fruitful discussions and comments on the manuscript, we thank colleagues from the Nutritional Physiology Unit (Technische Universität München, Freising, Germany), especially T. Zietek, J. Fiamoncini, J. Stolz and K. Gedrich.

**Funding** This study was financed by institutional funds of the ZIEL Research Center of Nutrition and Food Sciences.

**Duality of interest** The authors declare that there is no duality of interest associated with this manuscript.

**Contribution statement** PG, BS, and HD contributed to conception and design of the study. PG, IP and DR were responsible for the acquisition and analysis of metabolite profiling data. PG and JE were responsible for the acquisition and analysis of mRNA expression data. PG, IP, DR and ASH were responsible for acquisition of human plasma data. PG and HD drafted and wrote the manuscript. All authors contributed to critical revision of the manuscript and approved the final version. HD is the guarantor of this work.

## References

- Menni C, Fauman E, Erte I et al (2013) Biomarkers for type 2 diabetes and impaired fasting glucose using a nontargeted metabolomics approach. *Diabetes* 62:4270–4276
- Felig P, Marliss E, Cahill GF Jr (1969) Plasma amino acid levels and insulin secretion in obesity. *N Engl J Med* 281:811–816
- Roberts LD, Koulman A, Griffin JL (2014) Towards metabolic biomarkers of insulin resistance and type 2 diabetes: progress from the metabolome. *Lancet Diabetes Endocrinol* 2:65–75
- Newgard CB, An J, Bain JR et al (2009) A branched-chain amino acid-related metabolic signature that differentiates obese and lean humans and contributes to insulin resistance. *Cell Metab* 9:311–326
- Coleman DL (1978) Obese and diabetes: two mutant genes causing diabetes-obesity syndromes in mice. *Diabetologia* 14:141–148
- Coleman DL, Hummel KP (1973) The influence of genetic background on the expression of the obese (*Ob*) gene in the mouse. *Diabetologia* 9:287–293
- R Development and Core Team (2008) A language and environment for statistical computing. Available from [www.R-project.org](http://www.R-project.org), accessed 8 Apr 2015
- Hoefle AS, Bangert AM, Stamford A et al (2015) Metabolic responses of healthy or prediabetic adults to bovine whey protein and sodium caseinate do not differ. *J Nutr* 145:467–475
- Ecker J, Liebisch G, Englmaier M, Grandl M, Robenek H, Schmitz G (2010) Induction of fatty acid synthesis is a key requirement for phagocytic differentiation of human monocytes. *Proc Natl Acad Sci U S A* 107:7817–7822
- Nikiforova VJ, Giesbertz P, Wiemer J et al (2014) Glyoxylate, a new marker metabolite of type 2 diabetes. *J Diabetes Res* 2014:9
- Devereux Woods D (1935) Indole formation by *Bacterium coli*: the breakdown of tryptophan by washed suspensions of *Bacterium coli*. *Biochem J* 29:640–648
- Padberg I, Peter E, Gonzalez-Maldonado S et al (2014) A new metabolomic signature in type-2 diabetes mellitus and its pathophysiology. *PLoS One* 9: e85082
- Kawano Y, Cohen DE (2013) Mechanisms of hepatic triglyceride accumulation in non-alcoholic fatty liver disease. *J Gastroenterol* 48:434–441
- Biddinger SB, Miyazaki M, Boucher J, Ntambi JM, Kahn CR (2006) Leptin suppresses stearoyl-CoA desaturase 1 by mechanisms independent of insulin and sterol regulatory element-binding protein-1c. *Diabetes* 55:2032–2041
- Brown MS, Goldstein JL (2008) Selective versus total insulin resistance: a pathogenic paradox. *Cell Metab* 7:95–96
- Wang Y, Botolin D, Xu J et al (2006) Regulation of hepatic fatty acid elongase and desaturase expression in diabetes and obesity. *J Lipid Res* 47:2028–2041
- Tvrđik P, Westerberg R, Silve S et al (2000) Role of a new mammalian gene family in the biosynthesis of very long chain fatty acids and sphingolipids. *J Cell Biol* 149:707–718
- Shimano H, Horton JD, Hammer RE, Shimomura I, Brown MS, Goldstein JL (1996) Overproduction of cholesterol and fatty acids causes massive liver enlargement in transgenic mice expressing truncated SREBP-1a. *J Clin Invest* 98:1575–1584
- Horton JD, Shimomura I, Brown MS, Hammer RE, Goldstein JL, Shimano H (1998) Activation of cholesterol synthesis in preference to fatty acid synthesis in liver and adipose tissue of transgenic mice overproducing sterol regulatory element-binding protein-2. *J Clin Invest* 101:2331–2339
- Bjorntorp P, Bergman H, Varnauskas E (1969) Plasma free fatty acid turnover rate in obesity. *Acta Med Scand* 185:351–356
- Frayn KN (2002) Adipose tissue as a buffer for daily lipid flux. *Diabetologia* 45:1201–1210

22. Funai K, Song H, Yin L et al (2013) Muscle lipogenesis balances insulin sensitivity and strength through calcium signaling. *J Clin Invest* 123:1229–1240
23. Paiva H, Lehtimäki T, Laakso J et al (2003) Plasma concentrations of asymmetric-dimethyl-arginine in type 2 diabetes associate with glycemic control and glomerular filtration rate but not with risk factors of vasculopathy. *Metab Clin Exp* 52:303–307
24. Akanuma Y, Morita M, Fukuzawa N, Yamanouchi T, Akanuma H (1988) Urinary excretion of 1,5-anhydro-D-glucitol accompanying glucose excretion in diabetic patients. *Diabetologia* 31:831–835
25. Baxmann AC, Ahmed MS, Marques NC et al (2008) Influence of muscle mass and physical activity on serum and urinary creatinine and serum cystatin C. *Clin J Am Soc Nephrol* 3:348–354
26. Muñoz GE, Marshall SH (1992) Free L-phosphotyrosine activates human platelets: molecular evidence for a new signal transducer. *Cell Mol Biol* 38:629–633
27. Gresele P, Marzotti S, Guglielmini G et al (2010) Hyperglycemia-induced platelet activation in type 2 diabetes is resistant to aspirin but not to a nitric oxide-donating agent. *Diabetes Care* 33:1262–1268
28. Sainz N, Rodriguez A, Catalan V et al (2009) Leptin administration favors muscle mass accretion by decreasing FoxO3a and increasing PGC-1alpha in ob/ob mice. *PLoS One* 4: e6808
29. She P, Van Horn C, Reid T, Hutson SM, Cooney RN, Lynch CJ (2007) Obesity-related elevations in plasma leucine are associated with alterations in enzymes involved in branched-chain amino acid metabolism. *Am J Physiol Endocrinol Metab* 293:E1552–E1563
30. Shin AC, Fasshauer M, Filatova N et al (2014) Brain insulin lowers circulating BCAA levels by inducing hepatic BCAA catabolism. *Cell Metab* 20:898–909
31. Wang-Sattler R, Yu Z, Herder C et al (2012) Novel biomarkers for pre-diabetes identified by metabolomics. *Mol Syst Biol* 8:615
32. Horning MG, Martin DB, Karmen A, Vagelos PR (1961) Fatty acid synthesis in adipose tissue. II. Enzymatic synthesis of branched chain and odd-numbered fatty acids. *J Biol Chem* 236:669–672